Research article

Open Access

Malignant myoepithelial cells are associated with the differentiated papillary structure and metastatic ability of a syngeneic murine mammary adenocarcinoma model

Viviana Bumaschny, Alejandro Urtreger, Miriam Diament, Martín Krasnapolski, Gabriel Fiszman, Slobodanka Klein and Elisa Bal de Kier Joffé

Research Area, Institute of Oncology 'Angel H. Roffo', University of Buenos Aires, Argentina

Corresponding author: Elisa Bal de Kier Joffé (e-mail: elisabal@fmed.uba.ar)

Abstract

Background: The normal duct and lobular system of the mammary gland is lined with luminal and myoepithelial cell types. Although evidence suggests that myoepithelial cells might suppress tumor growth, invasion and angiogenesis, their role remains a major enigma in breast cancer biology and few models are currently available for exploring their influence. Several years ago a spontaneous transplantable mammary adenocarcinoma (M38) arose in our BALB/c colony; it contains a malignant myoepithelial cell component and is able to metastasize to draining lymph nodes and lung.

Methods: To characterize this tumor further, primary M38 cultures were established. The low-passage LM38-LP subline contained two main cell components up to the 30th subculture, whereas the higher passage LM38-HP subline was mainly composed of small spindle-shaped cells. In addition, a large spindle cell clone (LM38-D2) was established by dilutional cloning of the low-passage MM38-LP cells. These cell lines were studied by immunocytochemistry, electron microscopy and ploidy, and syngeneic mice were inoculated subcutaneously and intravenously with the different cell lines, either singly or combined to establish their tumorigenic and metastatic capacity.

Results: The two subpopulations of LM38-LP cultures were characterized as luminal and myoepithelium-like cells, whereas LM38-HP was mainly composed of small, spindle-shaped epithelial cells and LM38-D2 contained only large myoepithelial cells. All of them were tumorigenic when inoculated into syngeneic mice, but only LM38-LP cultures containing both conserved luminal and myoepithelial malignant cells developed aggressive papillary adenocarcinomas that spread to lung and regional lymph nodes.

Conclusion: The differentiated histopathology and metastatic ability of the spontaneous transplantable M38 murine mammary tumor is associated with the presence and/or interaction of both luminal and myoepithelial tumor cell types.

Keywords: ductal papillary adenocarcinoma, lymph node metastasis, mammary cancer cell lines, myoepithelium, proteases

Introduction

Two epithelial cell types, present in roughly equal numbers, line the normal duct and lobular system of the mammary gland. There is an inner 'luminal' or 'secretory' cell layer surrounded by an outer myoepithelial cell layer. Thus myoepithelial cells, interposed between stroma and lumen, are placed in an ideal location to control many aspects of luminal function such as polarity, electrolyte and fluid flow, and response to endocrine or paracrine signals [1,2].

The contribution of myoepithelial cells to benign and malignant pathologies has only recently been recognized. Some studies have attributed great significance to the normal myoepithelium as a paracrine inhibitor of mammary cell proliferation and morphogenesis [3,4], invasion [5],

---

α-SMA = α-smooth muscle actin; CK14 = cytokeratin 14; CM = conditioned media; FCS = fetal calf serum; MMP = matrix metalloproteinase; pan-CK = pancytokeratins; PBS = phosphate-buffered saline; s.c. = subcutaneous(ly); uPA = urokinase-type plasminogen activator.

and angiogenesis [6], and thus as an inhibitor of tumor progression [7]. Nevertheless, the role of malignant myoepithelial cells remains a major enigma in breast cancer biology.

Tumors showing myoepithelial differentiation are rarely composed of a single cell type as in pure myoepitheliomas or myoepithelial carcinoma. More often, myoepithelial cells coexist with neoplastic luminal epithelial cells in adenoid cystic carcinoma, adenosquamous carcinoma, adenomyo-epithelioma, and poorly differentiated myoepithelium-rich carcinoma. Although these are rather common tumors in dogs, rats, and mice [8], they are considered rare in human clinical practice, and reports in the literature are generally of small series or isolated case reports [9]. Furthermore, the contribution of myoepithelial cells to human ordinary ductal carcinomas is also unclear. Interestingly, some reports suggest that 2–18% of so-called ductal carcinomas – no special type – show focal or diffuse myoepithelial differentiation by immunohistochemical criteria [10,11], and about 50% of these exhibit aggressive malignant behavior [9].

Several observations favor the existence of bipotent mammary cell precursors giving rise to both luminal and myoepithelial cells [2]. However, the precise location and molecular markers of mammary precursor cells, and also their role in mammary carcinogenesis, are still a matter of controversy. Although it has been proposed that the myoepithelial cell might derive from precursors within the luminal layer [12], a recent study [13] has identified a new cell population, a precursor of both cell types, within the human breast. Moreover, Gudjonsson and colleagues [14] have isolated a bipotent progenitor cell located in the suprabasal compartment *in vivo*. Recent work employing laser capture and comparative genomic hybridization analysis on human pure myoepithelial carcinomas and ductal carcinomas of no special type [15] suggest that the first genetic alterations probably occur in a common stem cell, followed by further changes in the lineage-committed cell progenitors.

Most murine models for breast cancer development, although extremely useful, have some characteristics that might preclude the extrapolation of results to the human disease [16]. In particular, even though lymph nodes represent the first and most frequent metastatic site in human breast cancer, murine mammary tumors usually do not metastasize to the regional lymph nodes. However, several years ago a spontaneous transplantable mammary adeno-carcinoma (M38) showing the capacity to metastasize both to draining lymph nodes and lung arose in our BALB/c colony [17]. Here we describe the establishment and characterization of cell sublines from the murine M38 mammary tumor. Our results show that this new murine mammary tumor model is composed of two subpopulations of tumor cells with luminal and myoepithelium-like

phenotypes, and that its differentiated histopathology and pathogenic behaviour might depend on the presence and/or interaction of both cell types.

Materials and methods
Tumor
M38 mammary tumor appeared spontaneously in the mammary gland of a pregnant BALB/c female mouse of our breeding colony in 1994. It was diagnosed as a well-differentiated ductal papillary adenocarcinoma [17]. Since then the M38 tumor has been maintained by subcutaneous (s.c.) serial transplantation to the flanks of either male or female syngeneic mice. M38-bearing mice still develop differentiated papillary tumors, and lung and lymph node metastases continue to develop in 100% and 88% of the cases, respectively.

Cell culture
The primary cell suspension was obtained by enzymatic digestion of M38 tumor fragments with 0.01% Pronase (Sigma, St Louis, MO) and 0.0035% DNAse (Sigma) in IMDM/F12 medium (Life Technologies Inc., Gaithersburg, MD, USA). Cells were cultured in IMDM/F12 medium supplemented with 10% fetal calf serum (FCS; Natacor, Córdoba, Argentina) and 2 mM L-glutamine (Sigma) at 37°C in plastic flasks (Nunc, Roskilde, Denmark) in a humidified 5% CO_2/air atmosphere. Serial passages were made by treatment of confluent monolayers with 0.25% trypsin and 0.02% EDTA in Ca^{2+}-free and Mg^{2+}-free PBS. Once established, the continuous LM38 cell line was maintained in the conditions mentioned above. Cells were determined periodically to be mycoplasma-free by Hoechst's method.

During subculture the LM38 cell line acquired important phenotypic changes. Thus, two different sublines were defined for further characterization: low-passage LM38 cells (LM38-LP; passages 7–15) and high-passage LM38 cells (LM38-HP; passages 55–65).

A third subline, LM38-D2, was cloned from the different cell subpopulations present in the LM38-LP subline by limiting dilution as described previously [18].

Cell growth
Cell suspensions (2 ml) containing 1.2×10^5 viable cells/ml were seeded in triplicate to 35 mm plastic dishes (Nunc) in medium supplemented with 10% FCS and 2 mM L-glutamine. Fresh medium was replaced every 24 hours. Cultures were harvested at 24, 48, 72 and 96 hours after seeding, and cell growth was evaluated by treatment with trypsin and subsequent cell counting in the presence of trypan blue. The population doubling time was calculated from the exponential phase of growth curves. Susceptibility to nutrient depletion was also analyzed by culturing semiconfluent monolayers in serum-free medium.

Clonogenicity

Clonal cell growth was studied as described previously [19]. In brief, monodispersed cells were seeded at low density (500–5000 cells per dish) on 35 mm plastic dishes in complete medium. Medium was changed each 72 hours. After 8 days of culturing, plates were washed, fixed with 5% acetic acid in methanol, and stained with hematoxylin; the number of colonies was counted under an inverted microscope. Plating efficiency was defined as the percentage of cells able to grow as colonies of more than 10 cells.

Anchorage-independent spheroid formation

Monodispersed cell suspensions (2×10^5 cells/ml) in 10 ml of growth medium were seeded on a 100 mm Petri dish previously covered with a 1% agar-medium underlay to prevent cell attachment. In these conditions cells formed aggregates (spheroids) that were fixed for histological studies or trypsin-treated after various periods, stained with trypan blue and counted for growth evaluation.

Ploidy

To further characterize the cell components of the different LM38 cultures, 10^5 cells were seeded in triplicate wells of a tissue culture chamber slide (Lab-TekR; Nunc). After 72 hours, monolayers were fixed and stained with Feulgen for DNA content evaluation with an Image Analyzer Microscope CAS 200 (Cell Analysis Systems Inc., San Diego, CA, USA). At least 200 cells were analyzed for each culture.

Immunocytochemistry

Semiconfluent monolayers grown on glass coverslips or in Lab-Tek assemblies in complete medium were fixed with 5% acetic acid in methanol, then rehydrated, washed with PBS, blocked for endogenous peroxidase activity, and incubated overnight with 1:200 dilutions of monoclonal antibodies against pancytokeratins (pan-CK; a 20:1 mixture of clones AE1/AE3 recognizing cytokeratins 2, 4, 5, 6, 8, 10, 14, 15, 16 and 19; BioGenex Laboratories, San Ramon, CA, USA), cytokeratin 14 (CK14; clone NLC-LL002; Novo-Castra, Newcastle upon Tyne, UK), vimentin (clone V9; Dako, Carpinteria, CA), or α-smooth muscle actin (α-SMA; clone 1A4; Dako). Slides were then incubated with a biotinylated secondary antibody, washed, and incubated with a streptavidin–horseradish peroxidase conjugate (Vector Laboratories, Burlingame, CA, USA). Antigens were revealed with 7% diaminobenzidine and 3% H_2O_2 in PBS, and nuclei were counterstained with Harris hematoxylin. For E-cadherin (Clone 36; Transduction Laboratories, Lexington, KY) expression cell cultures were revealed with a secondary antibody labeled with tetramethylrhodamine β-isothiocyanate. Actin cytoskeleton was studied by staining the same cell monolayers with phalloidin–fluorescein isothiocyanate.

Appropriate controls included the omission of the primary antibody and the substitution of purified mouse non-immune immunoglobulins at the same concentration as the first antibody. To avoid cross-reactions with endogenous murine IgGs, dilution of antibodies was performed in a buffer containing 2% normal mouse serum. Photographs were taken with a Nikon fluorescence biological microscope (Eclipse E400; Nikon, Tokyo, Japan) using either Kodak 100 film or a Nikon Coolpix digital camera.

Preparation of conditioned media (CM)

To prepare CM, semiconfluent monolayers growing in 35 mm plastic Petri dishes were washed extensively with PBS to eliminate traces of serum. Serum-free medium (1 ml) was added and the incubation was continued for 24 hours. CM were individually harvested, the remaining monolayers were scraped into cold lysis buffer (1% Triton X-100 in PBS), and cell protein content was determined (Bio-Rad Protein Assay). CM samples, aliquoted and stored at −40°C, were used only once after thawing.

Quantification of urokinase-type plasminogen activator (uPA) activity by zymography and radial caseinolysis

Secreted uPA activity was analyzed in CM prepared from LM38 cells. Zymograms were performed as described previously [18,19], using sodium dodecyl sulfate (SDS)–9% separating and 4% stacking polyacrylamide gels, under non-reducing conditions. After electrophoresis, gels were washed with 2.5% Triton X-100 and incubated on the surface of a gel composed of 2.5% agarose (Byodinamics SRL, Buenos Aires, Argentina), 33 mg/ml dried skimmed milk as casein source, 2 μg/ml plasmin-free plasminogen (Chromogenix, Mondal, Sweden), and 0.2 M Tris-HCl (pH 8.0). To confirm uPA activity present in zymograms, the assay was performed in the presence of amiloride (1 mM). To quantify uPA activity, a radial caseinolytic method was employed [18,19]. Plasminogen-free casein–agarose gels were used to test plasminogen-independent activity. uPA activities were referenced to a standard urokinase curve ranging from 0.05 to 25 U/ml and normalized to the protein content of the original cell culture.

Matrix metalloproteinase (MMP) zymography

Gelatinolytic MMP activity was determined on substrate-impregnated gels as described previously [19]. In brief, samples were separated on SDS–9% polyacrylamide gels containing 1 mg/ml copolymerized gelatin (Difco, Detroit, MI) under non-reducing conditions, followed by two washes with 2.5% Triton X-100. Gels were then incubated for 30–48 hours at 37°C in 0.25 M Tris-HCl, 1 M NaCl, 25 mM $CaCl_2$ at pH 7.4, and stained with 0.5% Coomassie G 250 (Bio-Rad, Richmond, CA) in methanol/acetic acid/water (30:10:60). The clear lysed areas of the bands on the stained gels were measured with a GS-700 densitometer (Bio-Rad, Hercules, CA, USA). To confirm that the activity was specifically due to MMPs, 40 mM EDTA was added to the incubation buffer.

Animals

Randomized inbred 2–4-month-old female BALB/c mice, obtained from our Animal Care Area, were employed. Food and water were administered *ad libitum*. All animal studies were conducted in accordance with the NIH Guide for the Care and the Use of Laboratory Animals.

Tumorigenicity and spontaneous metastasis studies

Mice were inoculated s.c. in the left flank with 5×10^4 to 2×10^5 of the various cell lines in 0.2 ml of IMDM/F12 medium. For co-inoculation experiments, LM38-HP and LM38-D2 cells were seeded together in different proportions (2:1 and 3:1) and mixed cultures were incubated *in vivo* for 36 hours before s.c. inoculation (2×10^5 cells/mouse). Animals were analyzed for tumor growth and spontaneous lymph node and lung metastases as described previously [19]. In brief, latency was defined as the time between s.c. injection of tumor cells and the evidence of external tumors in 50% of mice. The mean of the two largest perpendicular diameters was recorded twice a week to evaluate tumor growth. Mice were killed 65 days after tumor inoculation. The number and size of surface lung nodules were determined under a dissecting microscope. Lymph nodes, liver, kidney, and spleen were examined for the presence of metastatic nodules.

Experimental lung metastasis assay

To study their ability to produce experimental lung metastases, 3×10^5 cells were injected into the tail vein of syngeneic mice ($n = 10$ for each cell type) with a 27-gauge needle. Mice were monitored daily and killed 21 days later. Lungs were removed and the number and size of superficial lung colonies were determined as described above. The viability of the inoculated cells, as determined by trypan blue exclusion, was more than 95% for all *in vivo* assays.

Histology

Fixed tissues and spheroids (see above) were embedded in paraffin, and 5 μm sections were either stained with hematoxylin and eosin or tested for the expression of pan-CK, α-SMA, or vimentin, as described above.

Electron microscopy

For electron microscopy, tumor tissues fixed in 10% glutaraldehyde were post-fixed in 1% osmium tetroxide in 0.1 M phosphate buffer and embedded in Maraglass 655 (Polysciences Inc, Warrington, PA). Thin sections were stained with 1% Azur II plus 1% methylene blue in water for 3–5 min, then examined and photographed with a light microscope. Ultramicrotome sections, contrasted with uranyl acetate and lead citrate, were examined and photographed with a Zeiss EM-9A transmission electron microscope.

Statistical analysis

All experiments were performed in triplicate unless otherwise indicated. The significance of differences between

Figure 1
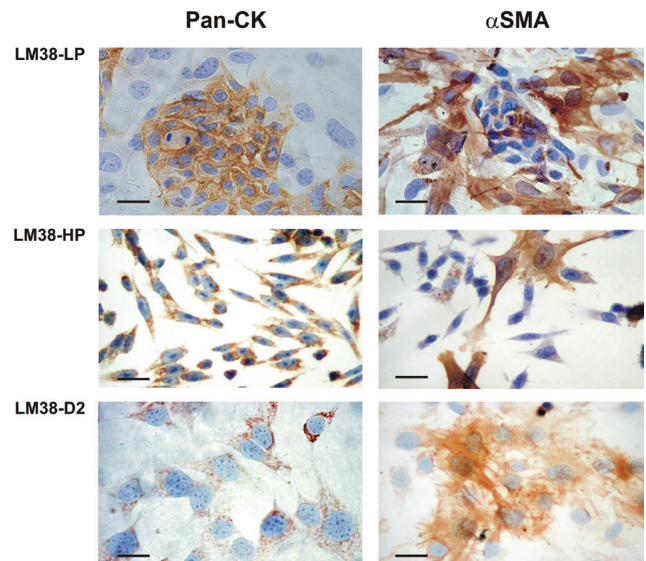
Immunocytochemical characterization of LM38-LP, LM38-HP, and LM38-D2 cells (top, middle, and bottom panels respectively). Cell monolayers were stained for the expression of pancytokeratins (pan-CK; left panels) and α-smooth muscle actin (α-SMA; right panels). The LM38-LP cell subline consisted mainly of islets of epithelial cells intensely positive for pan-CK surrounded by α-SMA-positive large myoepithelial cells. The LM38-HP subline predominantly showed small spindle cells positive for pan-CK, which do not form islets, and sparse α-SMA-positive altered myoepithelial cells. The LM38-D2 clone was homogenously made up of α-SMA-stained myoepithelial cells, also positive for pan-CK. (Original magnification ×400; scale bar, 35 μm.)

groups was calculated by applying Student's *t*-test or χ^2-test. The nonparametric Mann–Whitney *U*-test was employed to analyze differences in metastatic ability. A value of $P < 0.05$ was considered to be significant.

Results

Features and morphology *in vitro*

M38 primary cultures and the LM38-LP cell line (passages 7–15) were composed of two main subpopulations: islets of small cobblestone-like epithelioid cells surrounded by loosely arranged large and clear spindle cells with large nuclei (Fig. 1, top panels). In addition, limited numbers of less defined spindle cells were observed in the low-passage cultures. However, after about 30 passages the morphologic phenotype of the LM38 cells underwent a remarkable change, which remained stable for at least 75 subculture passages. LM38-HP cultures (passages 55–65) were mainly composed of small spindle cells that did not form tight cobblestone-like nests, together with occasional large spindle-shaped cells (Fig. 1, middle panels).

Single-cell cloning by limiting dilution of the heterogenous LM38-LP cell line resulted in the initial isolation of several clones of the large spindle cells with large nuclei, as well as some clones of small spindle cells and a few clones

forming epithelium-like islets. However, subpopulations with other morphologies always arose in these latter two groups after several days *in vitro* and a first subculture to amplify the clones. These clones ultimately contained small epithelial cells forming dense islets and/or large epithelial cells with a similar cobblestone appearance surrounded by large and light spindle cells (data not shown). We were therefore never able to isolate pure clones of epithelial cells forming islets by dilutional cloning. In contrast, clones that originally contained only large clear spindle cells continued to remain homogenous after repeated subcultures. One of these, LM38-D2, was employed for further characterization *in vitro* and *in vivo* (Fig. 1, bottom panels).

Immunocytochemistry was used to determine cell lineage. Islets of LM38-LP small epithelioid cells were intensely positive for pan-CK and negative for α-SMA (Fig. 1, upper panels), but only poorly positive for vimentin (data not shown). LM38-LP large spindle cells surrounding the islets showed remarkable fibrillar cytoplasmic staining for α-SMA and moderate to low staining for pan-CK (Fig. 1, top panels) but were poorly positive for vimentin (data not shown). These results indicate that LM38-LP cultures were formed from islets of luminal-like epithelial cells surrounded by peripheral myoepithelial cells.

LM38-HP small spindle cells were positive for both pan-CK and vimentin (data not shown), but negative for α-SMA (Fig. 1, middle panels). Sparse larger spindle cells were also found in LM38-HP cultures; they were smaller than those present in LM38-LP cultures and showed diffuse cytoplasmic staining and a less organized array of myofilaments by anti-α-SMA immunostaining (Fig. 1, middle panels). LM38-HP cultures were therefore mainly composed of epithelial cells with a remarkably undifferentiated morphological phenotype, and a secondary minor subpopulation of altered myoepithelial cells.

The clonal LM38-D2 cells showed fibrillar staining for α-SMA, and stained with variable intensities for pan-CK, thus indicating their myoepithelial lineage (Fig. 1, bottom panels).

For further characterization, the expression of E-cadherin and the organization of the actin cytoskeleton of the different cell sublines were also analyzed. The islets of small epithelial cells of LM38-LP cultures showed intense membrane staining for E-cadherin and a cortical distribution of actin, which is typical of an epithelial phenotype (Fig. 2). On the contrary, myoepithelial cells from LM38-LP subline and clone LM38-D2 myoepithelial cells did not express E-cadherin and presented a filamentous actin cytoskeleton forming stress fibers (Fig. 2). Interestingly, the small spindle cells of LM38-HP subline did not express E-cadherin and presented stress fibers in addition to some actin cortical distribution (Fig. 2), suggesting an epithelio-mesenchymal transition (EMT) of these cells.

Figure 2
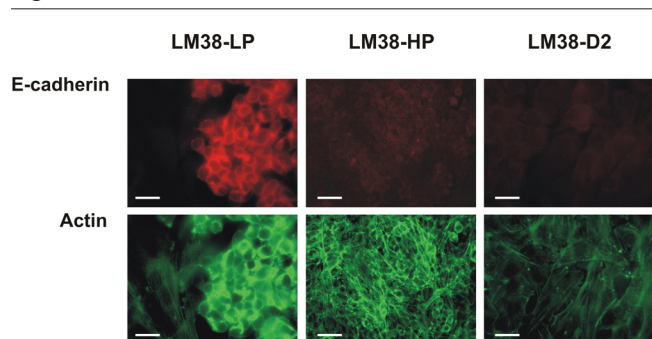
Dual staining for E-cadherin (upper panels) and actin (lower panels) of LM38-LP, LM38-HP, and LM38-D2 cells (left, middle, and right panels, respectively). Whereas islets of epithelial cells showed evident E-cadherin staining of membranes, neither myoepithelial cells (in LM38-LP or LM38-D2 cultures) nor LM38-HP epithelioid cells did so. Actin was distributed cortically in the islets of epithelial cells, formed long stress fibres in the myoepithelial cells, and showed poor cortical distribution and the simultaneous presence of stress fibers in the spindle-shaped LM38-HP cell line. (Original magnification ×400; scale bar, 35 μm.)

A summary of the main cytological features of LM38 sublines is presented in Table 1.

DNA ploidy analysis
To further identify the origin and evolution of the cellular components of LM38-LP, LM38-HP, and LM38-D2 cultures, the DNA content of cells was analyzed employing Feulgen staining and an image analyzer microscope. As shown in Fig. 3a, LM38-LP cultures contained two principal aneuploid subpopulations. The main one (47%), probably corresponding to the previously characterized large spindle myoepithelial cell compartment, was hypertetraploid with a DNA index of 2.75 (relative to 5.6 pg of DNA content in G1 somatic mouse cells). The subpopulation of cuboideal epithelial cells (27%) was hypotriploid with a DNA index of 1.35. LM38-HP cultures exhibited a main peak, corresponding to the population of small spindle cells (54.2%), with the same DNA index (1.35) already observed in the luminal epithelial cells of LM38-LP cultures, and a smaller (<20%) secondary peak of cells with a 2.75 DNA index, probably constituted both by epithelial cells undergoing the G2/M-phase and a small population of myoepithelial ones (Fig. 3b). All LM38-D2 cells presented a DNA index equal or higher than 2.75, quite similar to that of the LM38-LP myoepithelial subpopulation (Fig. 3c). These results indicate that both the luminal epithelial and myoepithelial cells are transformed.

Cell growth
Unsynchronized LM38-HP cells growing in monolayers in IMDM/F12 supplemented with 10% FCS had a remarkably shorter population doubling time as compared with the low-passage LM38-LP cells. In contrast, the LM38-D2

Table 1

Summary of cytological, histological and immunocytochemical features of LM38 sublines growing in monolayer culture, in suspension, or after subcutaneous inoculation *in vivo*

Feature	LM38-LP	LM38-HP	LM38-D2
Monolayer cultures			
Islets of epithelioid cells	Abundant	Absent	Absent
Pan-CK	+++		
Vimentin	+/−		
α-SMA	−		
E-cadherin	+		
Small spindle cells	Scarce	Abundant	Absent
Pan-CK	Not defined	++	
Vimentin	Not defined	+	
α-SMA	−	−	
E-cadherin	−	−	
Large spindle cells	Abundant	Scarce	Abundant[a]
Pan-CK	+	+	+
Vimentin	+/-	+/−	ND
α-SMA	+++	+/++	+++
E-cadherin	−	−	−
Spheroids	Yes	Yes	ND
Shape	Smooth, round	Irregular clusters	
Morphogenesis	Gland-like	Loose and solid cords	
Pan-CK	+++ polarized cells	++ intermingled cells	
α-SMA/CK14	+++ central, peripheral or isolated cells	+ intermingled cells	
Subcutaneous tumors	Papillary differentiated adenocarcinoma	Poorly differentiated adenocarcinoma	Undifferentiated (myoepithelioma-like)
Pan-CK	+++ abundant cells	+ or +/− scarce cells	ND
α-SMA	+++ abundant cells	+/− scarce cells	+++

[a]Pure cell type. α-SMA, α-smooth muscle actin; CK14 = cytokeratin 14; ND, not done; pan-CK, pancytokeratins.

clone grew at a slower rate than the parental LM38-LP line (Table 2). However, when seeded at low density under more stringent growth conditions, the LM38-LP cells exhibited a significantly higher plating efficiency than the LM38-HP cells (Table 2), suggesting an association between the decrease in clonogenic capacity and the loss or impairment of myoepithelial cells. Moreover, LM38-LP cells were more resistant than LM38-HP cells to serum starvation (Table 2).

To determine whether a soluble factor was responsible for the different growth patterns of our cells, LM38-HP cells were grown in the presence of filtered CM (25%, v/v) from LM38-LP cultures. No changes in their morphology or proliferation rate were evident even after 30 days of treatment. The same negative results were obtained after applying LM38-HP CM to LM38-LP monolayer cultures.

Anchorage-independent growth, and characterization of spheroids

LM38-LP and LM38-HP cultures began to form spheroids as soon as 24 hours after being seeded on an agar-medium layer. Whereas LM38-LP cells formed tight smooth-surfaced spheroids, LM38-HP aggregates were made up of loose cells resembling grape clusters rather than well-organized spheroids (Fig. 4). Cell counting revealed a steady increase in the number of LM38-HP cells over 9 days, whereas the number of LM38-LP cells remained stable for 4 days and then gradually decreased (Fig. 5).

Interestingly, histologic analysis revealed that most LM38-LP spheroids resembled glandular structures with a polarized epithelium (Fig. 4, left panels). In contrast, LM38-HP cells formed relatively large irregular clusters without polarization or lumen formation (Fig. 4, right panels).

Figure 3

(a)

(b)

(c)
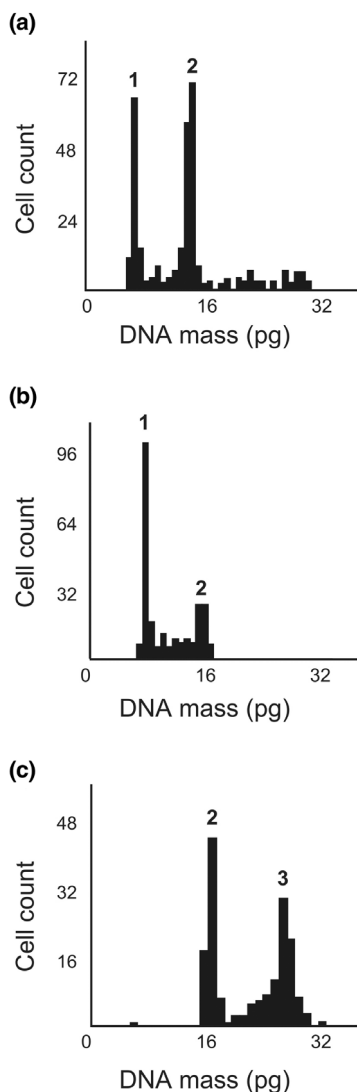
Analysis of DNA ploidy of LM38-LP **(a)**, LM38-HP **(b)** and LM38-D2 **(c)** cells. (a) Whereas islets of epithelial cells were hypotriploid (1), large spindle cells, probably of myoepithelial phenotype, made up a large hypertetraploid subpopulation (2). (b) The main small spindle cell subpopulation was hypotriploid (1), similarly to the islets of epithelial cells in LM38-LP cultures. A small peak of a hypertetraploid subpopulation was also found (2). (c) The myoepithelial LM38-D2 clone was made up of two subpopulations, either hypertetraploid (2) or even with a higher DNA index (3).

LM38-LP spheroids showed strong staining for pan-CK in the polarized epithelial cells, and poor expression of cytokeratin in the larger cells occupying the spheroid cores or loose within the culture (Fig. 4, upper panels). Staining for CK14, a cytokeratin specific for myoepithelial cells, showed positivity in cells found either in the core of the spheroids or intermingled with the polarized luminal cells or, sometimes, in cells organized as a basal epithelial layer in the periphery of the spheroid (Fig. 4, lower panels). Similar results were
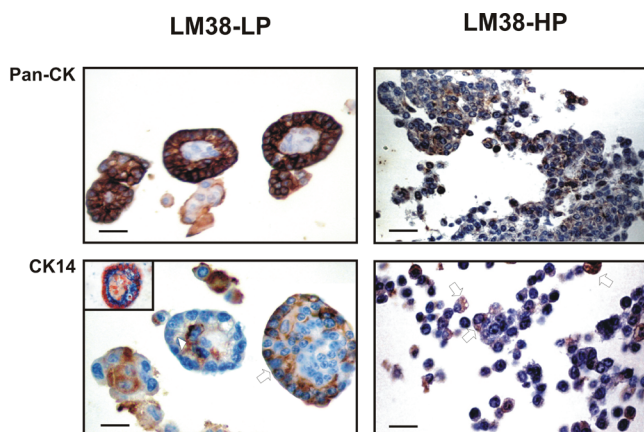
Table 2

Growth properties of LM38 *in vitro*

Property	LM38-LP	LM38-HP	LM38-D2
Population doubling time (h)	18 ± 1.1	10 ± 0.6*	33 ± 2.4*
Clonogenic growth (% of plating efficiency)	3.95 ± 0.8	0.43 ± 0.1*	ND
Survival (%) after 48 h serum starvation	65	31	ND

The representative data shown correspond to one of three independent experiments. ND, not done. *$P < 0.05$ compared with LM38-LP.

Figure 4

Morphology and cellular composition of spheroids formed in a three-dimensional growth assay. LM38-LP cells (left panels) formed glandular-like smooth-bordered spheroids, whereas LM38-HP cells (right panels) grew in loose irregular clusters. Cells positive for pancytokeratins (pan-CK; upper panels) formed a polarized epithelial layer surrounding a kind of lumen in LM38-LP spheroids, but were disorganized in LM38-HP clusters. In LM38-LP spheroids myoepithelial cells, stained for either cytokeratin 14 (CK14) or α-smooth muscle actin (α-SMA; lower panels), were found as a basal cell layer (arrow) surrounding luminal epithelial cells or occupying the spheroid core in an inside-out display (arrowhead). Some CK14-positive myoepithelial cells were found intermingled in LM38-HP clusters (arrow). Inset: Double staining of LM38-LP spheroids: α-SMA (light brown), pan-CK (blue), nuclei (red). (Original magnification ×400; scale bar, 35 μm.)

found when a double staining for cytokeratins and α-SMA was performed on the same section, revealing that myoepithelial tumor cells concomitantly expressed epithelial and smooth muscle markers whereas polarized luminal cells presented only a very high expression of cytokeratins (Fig. 4, inset). In contrast, moderate expression of cytokeratins was found in LM38-HP spheroids, and some cells, intermingled with negative ones, were positive for cytokeratin 14 (Fig. 4) or for α-SMA (data not shown).

These results show that only the heterogenous LM38-LP cultures had the capacity to acquire a highly differentiated

Figure 5
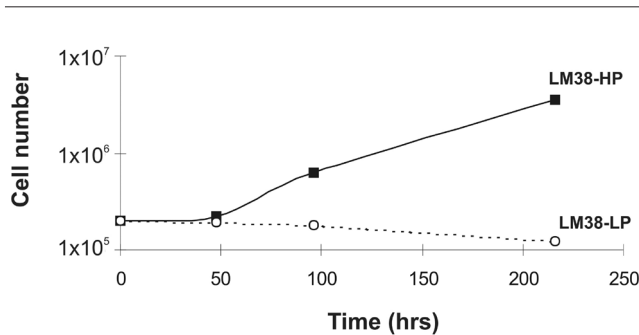
Growth curves of LM38 sublines in a three-dimensional assay in liquid medium. Cell suspensions (2 × 10⁵ cells/ml) in complete growth medium were seeded on top of an agar layer. At different time points spheroids were collected and trypsin-treated; cells were then counted. Whereas the LM38-HP cells proliferated at least up to the 10th day in this condition, the LM38-LP subline not only did not proliferate but began to die after the fourth day. The representative data shown correspond to one of two independent experiments. Standard deviations (not shown) were within ±10% of the mean.

histotypic morphology resembling glandular ducts when grown in suspension, forming spheroids made up from both cell types found in monolayers (Table 1).

Behavior *in vivo*

The LM38-LP and LM38-HP cultures, as well as the LM38-D2 clone, were analyzed for tumorigenicity and spontaneous metastatic potential after s.c. inoculation in the flanks of syngeneic BALB/c mice. As shown in Table 3, LM38-LP tumors exhibited a short latency, a high growth rate, and a high rate of metastasis to lung and lymph node, similar to that observed for the primary cultures of the parental M38 tumor (data not shown). In contrast, LM38-HP tumors had a longer latency and a remarkably slower growth rate, as well as a lower incidence of spontaneous lung and lymph node metastasis. Regarding tumorigenicity, whereas the inoculation of 5 × 10⁴ LM38-LP cells allowed tumor formation in 100%

of mice, only 30% of mice inoculated with the same number of LM38-HP cells showed tumor growth. LM38-D2 clone tumors had a longer latency, a slower growth rate than LM38-LP tumors, an extremely low rate of spontaneous spread to the lung, and no capacity for lymph node dissemination (Table 3).

The ability of the various cells to form experimental lung metastases after injection into a tail vein was also examined. As shown in Table 3, LM38-HP cells exhibited a remarkably lower ability to colonize lung as compared with LM38-LP cultures. Moreover, LM38-D2 cells consistently failed to form experimental lung metastasis.

Histopathology and ultrastructure

LM38-LP s.c. tumors were differentiated papillary adeno-carcinomas, with the same histopathology as the parental M38 tumor. These contained finger-like projections of fibrovascular stroma surrounded by heterogenous neo-plastic cells organized, as single or multilayered epithelia with papillary fronds and nodules, into lumina that were frequently occupied by multifocal apoptotic and necrotic foci (Fig. 6, upper left panel). Mitotic figures were frequently found in the tumor tissue. Tumors grew by invading the muscular and adipose layers of the subcutis, and at 60 days after inoculation tumor cells also invaded the dermis and the dermal papillae in some animals, causing visible ulceration on top of the tumors (data not shown). Whereas lymph node metastases replaced the whole normal tissue with the same papillary organization, lung metastases mainly formed solid cords accompanied with less vascular-connective tissue (Fig. 7).

LM38-HP s.c. tumors grew as solid and poorly differentiated carcinomas of homogenously small light cells, with little or no evidence of glandular or papillary differentiation (Fig. 6, upper middle panel). Only sparse small apoptotic foci and almost no local invasiveness (data not shown) were other characteristics of LM38-HP tumors. Lung metastases, although infrequent, were similar in appearance to the primary s.c. tumors (data not shown).

Table 3

Behavior of LM38 cell lines *in vivo*

Property	LM38-LP	LM38-HP	LM38-D2
Subcutaneous tumor latency [median (range); days]	5 (5–19)	19 (19–61)*	24.5 (18–69)*
Subcutaneous tumor growth rate (mean±SD; mm/day)	0.22±0.04	0.05±0.01*	0.11±0.02*
Incidence of spontaneous lung metastases (%)	9/9 (100)	4/8* (50)	1/8* (12.5)
Incidence of spontaneous lymph node metastases (%)	5/9 (55.5)	1/8* (12.5)	0/8* (0)
No. of experimental lung metastases [median (range)]	40.5 (9–80)	0 (0–3)*	0 (0–1)*

The representative data shown correspond to one of three independent experiments. Mice were inoculated with 2 × 10⁵ cells for subcutaneous tumor growth and assessment of spontaneous metastasizing ability, or with 3 × 10⁵ cells for the experimental metastasis assay. *$P < 0.05$ compared with LM38-LP.

Figure 6
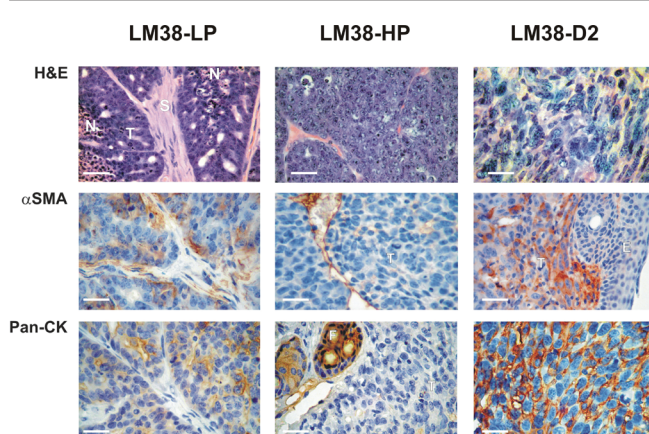
Histopathology of subcutaneous tumors formed after the inoculation of LM38 sublines into syngeneic mice. Tumor sections were stained with hematoxylin and eosin (upper panels) or by an immunohistochemistry procedure, for α-smooth muscle actin (α-SMA; middle panels), for pancytokeratins (pan-CK; left and central lower panels) or for cytokeratin 14 (CK14; right lower panel). The LM38-LP cells (left panels) formed differentiated papillary adenocarcinomas made up of cells positive for α-SMA and pan-CK surrounding fibrovascular strands. In contrast, the LM38-HP cells (central panels) formed poorly differentiated adenocarcinomas with no evidence of glandular structures, that were made up of cells mostly negative for both cell lineage markers. The LM38-D2 clone (right panels) grew as an undifferentiated tumor consisting of large cells positive for CK14 and α-SMA. (Original magnification ×400; scale bar, 35 μm.) E, epidermis; F, hair follicle; N, necrosis; S, fibrovascular stroma; T, tumor tissue.

Immunohistochemical staining for pan-CK revealed that LM38-LP tumors were strongly positive, whereas LM38-HP tumors showed minimal staining or were completely negative (Fig. 6, lower panels). No tumor cell expressed vimentin *in vivo* (data not shown). Interestingly, the presence of abundant α-SMA-positive myoepithelial cells was evident in the parenchyma of LM38-LP s.c. tumors and lymph node metastases, but not in LM38-HP tumors (Fig. 6, middle panels and Fig. 7a,c). α-SMA is a reliable differentiation marker that is expressed exclusively in smooth muscle and in myoepithelial cells. α-SMA-positive myoepithelial cells were mainly found in contact with the stroma, forming several layers, and also mixed at random with α-SMA-negative luminal epithelial cells (Fig. 6). Myoepithelial cells could be also found invading the stroma, but could be differentiated morphologically from myofibroblasts, which are also positive for α-SMA. Lung metastases were mainly composed of cells positive for pan-CK with only occasional intermingled α-SMA-positive cells (Fig. 7b,d).

The LM38-D2 clone formed highly undifferentiated solid tumors, with few apoptotic or necrotic foci, that were composed of large spindle-shaped CK14 and α-SMA-positive myoepithelial cells organized in broad strands or whorls (Fig. 6, right panels). Interestingly, in spite of their rather

Figure 7
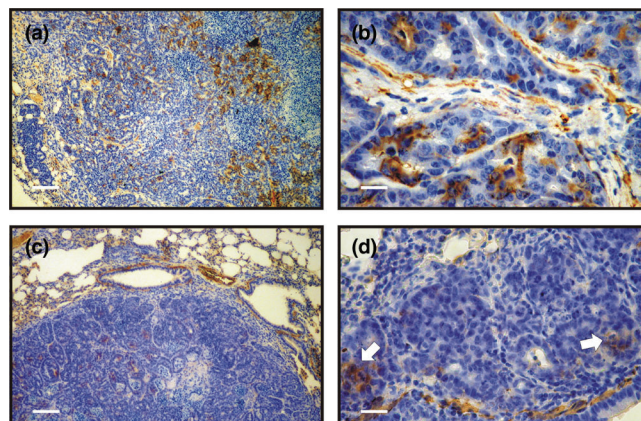
Immunohistochemical staining for α-smooth muscle actin (α-SMA) expression in LM38-LP lymph node **(a, b)** and lung metastases **(c, d)**. Whereas the lymph node metastasis showed the same histoarchitecture as the subcutaneous primary tumor, and the presence of many α-SMA-positive myoepithelial cells, lung metastatic nodes were less differentiated and only a few α-SMA positive cells could be found (arrow). Scale bars, 140 μm (a,c) and 35 μm (b,d).

slow growth rate and almost null metastatic ability, LM38-D2 tumors invaded the s.c. and adipose tissue, migrated through the s.c. skeletal muscle layer and reached the dermis (Fig. 6, right middle panel).

Histopathologic and immunohistochemical features of the different tumors are summarized in Table 1.

Tumors were also fixed and stained for transmission electron microscopy. As shown in Fig. 8a, light microscopy of Maraglass-embedded sections confirmed that heterogenous LM38-LP tumor parenchyma was composed of two main cell types: small epithelial cells of light cytoplasm and euchromatic nuclei with some dense chromatin granules placed adjacent to the lumen, and several layers of spindle dark cells with intensely stained irregular nuclei, located either close to the stroma or intermingled. In contrast, LM38-HP tumors were mainly formed from small light epithelial cells; only scanty dark cells were found either at the epithelium–stroma interface or mixed in the cellular cords (Fig. 8b). Several stages of cell differentiation, similar to those described in the epithelial renewal of the normal mouse mammary gland [20], were found in both LM38-LP and LM38-HP tumors.

Electron microscopy of neoplastic epithelial cells showed a paucity of cytoplasmic organelles, abundant free ribosomes and altered mitochondria. Nuclei could be either small and pale with heterochromatin, or large and euchromatic with distinct nucleoli. Neoplastic myoepithelial cells showed indented and densely stained heterochromatic nuclei, a dark pleomorphic cytoplasm with altered mitochondria, and

Figure 8
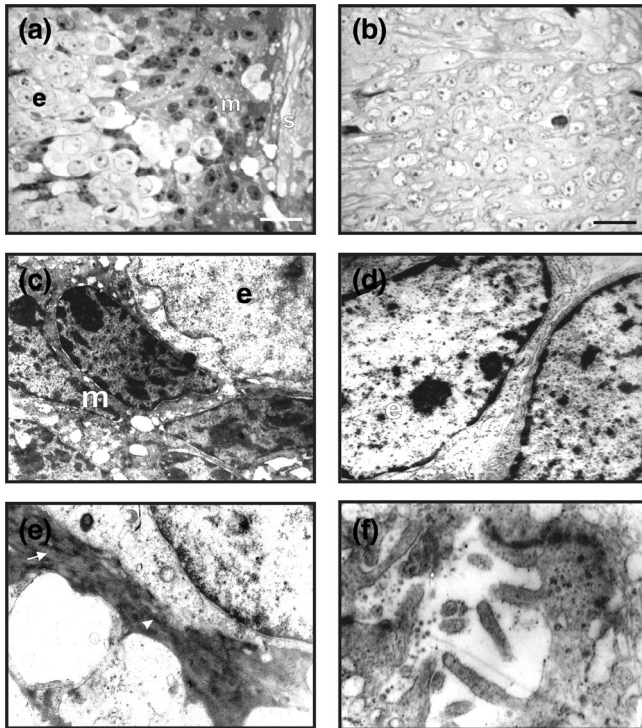
Morphological and ultrastructural features of LM38-LP and LM38-HP subcutaneous tumors. Light microscopy of Maraglass-embedded sections confirmed that LM38-LP **(a)** heterogenous tumor parenchyma was composed of two main cell types: small epithelial cells (e) of light cytoplasm and euchromatic nuclei with distinct nucleoli and some dense chromatin granules found close to the lumen, and basal myoepithelial (m) dark cells with intensely stained irregular nuclei and large nucleoli, placed near the stroma (s) or mixed at random with the small light cells. The LM38-HP tumors **(b)** were mainly made up of small light epithelial cells. (Original magnification ×400; scale bar, 35 μm.) Electron micrographs of LM38-LP tumor showing the two subpopulations at low magnification **(c)** (original magnification ×8000), a detail of the characteristic nuclei, nucleoli and cytoplasm of the light epithelial cells **(d)** (original magnification ×14,000) and the presence of abundant parallel microfilament bundles (arrow) and focal densities (arrowhead) in a cytoplasmic process of a dark myoepithelial cell **(e)** (original magnification ×17,000). Glandular lumina with microvilli and rudimentary intercellular junctions in LM38-HP tumor **(f)** (original magnification ×40,000), confirming its glandular epithelial origin.

abundant parallel microfilament bundles and irregular focal densities within long cytoplasmic processes (Fig. 8c–e). The glandular–epithelial origin of the poorly differentiated LM38-HP tumors was confirmed with the finding of both intracytoplasmic and conspicuous glandular lumina with microvilli and rudimentary intercellular junctions (Fig. 8f).

Production of proteases associated with tumor invasion
To seek an explanation of the differences in the metastatic capacity of our different cell subpopulations, we analyzed the production of uPA and MMPs, proteases associated with the invasive and metastatic phenotypes [21]. The LM38-HP cells and LM38-D2 clone secreted significantly less uPA than LM38-LP cells, as indicated by radial caseinolysis assays (Fig. 9a). Casein–plasminogen zymograms revealed that each of the cell lines secreted a main 48 kDa plasminogen activator (Fig. 9b) that could be inhibited by the specific uPA inhibitor amiloride, thus confirming its identity as uPA. These gels also confirmed the differential activity observed by the radial assay.

Regarding metalloproteinases, it was found that all LM38 sublines secreted considerable amounts of latent MMP-9, whereas only the highly metastatic LM38-LP cells were able to secrete limited amounts of latent MMP-2 to the culture medium (Fig. 9b).

Effect of the co-inoculation of LM38-HP and LM38-D2 cells on behaviour *in vivo*
To analyze whether the interplay between myoepithelial and epithelial cells was contributing to the behaviour of M38 mammary tumor *in vivo*, co-inoculation experiments were designed. Before the s.c. injection, LM38-HP and LM38-D2 cells were seeded in different proportions (2:1 and 3:1) and cultivated together for about 36 hours. Because no differences were found between the experiments, results are described together. We found that tumors resulting from the combination of cell lines were more invasive, grew faster (2.8-fold) and had a higher incidence and number of lung metastasis than LM38-HP and LM38-D2 tumors (Fig. 10, and data not shown). Metastasis size was also increased (data not shown). However, they did not recover either the ability to colonize the regional lymph node or the papillary differentiated histopathology (Fig. 10).

Discussion
Mouse models afford an excellent opportunity to improve our understanding of the natural biology of breast cancer. However, although exciting similarities can be found between human breast cancer and murine breast cancer models, important differences also exist. In particular, the fact that most murine mammary tumors metastasize to lung but do not form secondary tumors at the lymph node level is a matter of concern for most basic cancer researchers. In the past few years a panel of genetically engineered mouse models have been generated that could rapidly address these differences [16]. However, there are almost no spontaneous syngeneic mouse models available with which to study regional lymph node dissemination, even though it is the first and most frequent mode of dissemination for human breast cancer.

M38 is a mammary gland tumor that arose spontaneously in a pregnant mouse from our BALB/c colony. In addition to forming lung metastases after serial s.c. transplantation, M38 transplants formed secondary regional lymph node tumors in about 90% of the transplanted mice. From the first *in vivo* passages, the M38 tumor has also retained a differentiated papillary structure that is evident both in
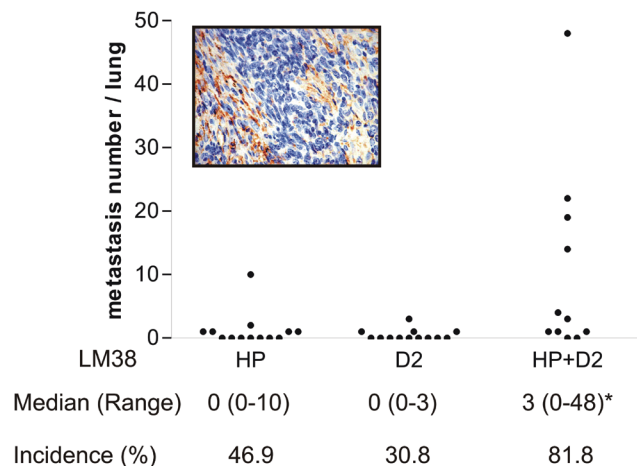
Figure 9

(a)

(b)
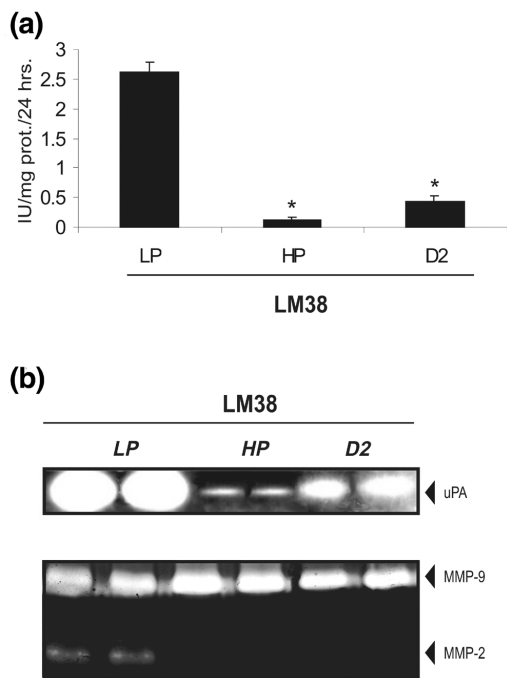
Secretion of proteases *in vitro* by the LM38 sublines. **(a)** Quantification of secreted urokinase-type plasminogen activator (uPA) activity by radial caseinolysis. The LM38-HP cells and LM38-D2 clone secreted significantly less uPA than LM38-LP cells. **(b)** Upper panel: zymogram of media conditioned by LM38-LP, LM38-HP, and LM38-D2 cells showing a main 48 kDa uPA band, confirming the differential activity observed in the radial assay. Lower panel: gelatin co-polymerized zymogram showing that only the highly metastatic LM38-LP cells were able to secrete matrix metalloproteinase (MMP)-2 to the culture medium. *$P < 0.05$ compared with LM38-LP.

Figure 10

LM38	HP	D2	HP+D2
Median (Range)	0 (0-10)	0 (0-3)	3 (0-48)*
Incidence (%)	46.9	30.8	81.8

Co-inoculation experiments *in vivo*. LM38-HP and LM38-D2 cells were cultivated together before subcutaneous injection, as described in the Materials and methods section. The combined tumors showed a higher incidence and number of spontaneous lung metastases than LM38-HP or LM38-D2 tumors. The results of two separate experiments are presented together. *$P < 0.05$ compared with LM38-HP and LM38-D2. Inset: a representative subcutaneous combined tumor stained for α-smooth muscle actin. Although myoepithelial cells surround epithelial cell nests, the characteristic papillary organization of M38 and LM38-LP tumors is not found.

primary s.c. tumors and lymph node metastases, but not in lung metastases which are solid and poorly differentiated. Papillary adenocarcinomas, infrequent carcinomas of the mammary gland in women, have been associated with a rather high incidence (32%) of lymph node metastases [22].

To characterize the M38 tumor further, we initiated primary monolayer cultures. Whereas other murine mammary tumor cultures that we have established contained a main epithelium-like population [19], both M38 primary cultures and the LM38-LP cell line were composed of two main populations: one forming cobblestone epithelium-like islets and the other being large clear spindle cells distributed around and between the islets. These cells closely resembled the cell components described in primary cultures of normal mammary gland epithelium, of either murine or human origin [23]. Coincident with those findings, the main LM38-LP cell components were identified as of luminal epithelial or myoepithelial lineages, with the aid of a panel of immunohistochemical markers. Although DMBA-induced murine mammary tumors containing both

luminal and myoepithelial cells have been described [8], murine spontaneous tumor models of a bicellular phenotype are lacking, and the reproducible development of matched pairs of malignant luminal and myoepithelial syngeneic cell lines has remained a major challenge in breast tumor biology and pathology.

It is accepted that tumors are composed of both malignant and adjacent normal cells. In fact, several years ago, Petersen and van Deurs [24] presented clear evidence that islets of 'normal' epithelial and myoepithelial cells of ductal origin could be found entrapped in primary monolayer cultures from human breast carcinomas, intermingled with islets of carcinoma cells. Moreover, the isolation of an immortal and severely aneuploid, but non-carcinogenic, cell line from a breast carcinoma biopsy was recently reported [25]. This is not true of the LM38 cell line: several lines of evidence presented here show incontrovertibly that all the cellular components were neoplastic, particularly their consistent and significant aneuploidy and their capacity to form tumors when injected into syngeneic mice, either as subpopulations of the heterogenous LM38-LP cell line or as isolated cloned cells.

Although the contribution of myoepithelial cells to benign and some malignant pathologies is recognized, this cell type has been largely neglected in molecular and biological studies. The erroneous concept that its role in

mammary gland physiology is confined to its contractile function in lactation and the belief that most human breast cancers arise from luminal epithelial cells explain this omission in part [1]. However, growing evidence supports its broader biological significance and its potential usefulness for understanding breast carcinogenesis. Thus, two recent reports [26,27], which analyze the gene expression profiles of breast carcinomas with a DNA microarray technology, have associated the estrogen receptor-positive status with a luminal phenotype, whereas arrays of estrogen receptor-negative tumors, with a worse prognosis, resemble those of myoepithelial basal cells.

Interestingly, we found that only LM38-LP cultures, upon s.c. inoculation, were able to develop into differentiated ductal papillary tumors with the characteristic fibrovascular stroma and parenchymatous luminal and myoepithelial cells. It is also important to note that lymph node metastases, but not lung metastases, exhibited the same papillary architecture and immunological staining as the s.c. tumor. In contrast, s.c. injection of the LM38-HP cell line, composed of a predominant small spindle epithelial subpopulation and a minor subpopulation of morphologically altered myoepithelial cells, resulted in the formation of undifferentiated solid carcinomas with a poor stroma. Moreover, we found that LM38-D2, the pure myoepithelial cell clone, was able to grow as s.c. tumors that resembled sarcomas by exhibiting a typical organization in broad whorls of the CK14-positive and α-SMA-positive spindle large cells, quite like that described previously for myoepithelial carcinomas, and different from that of tumors derived from luminal cells [9]. The histopathology of tumors grown after the co-inoculation of LM38-HP and LM38-D2 cells revealed spatial proximity between the epithelial and myoepithelial cells that was not enough to result in a papillary organization. Our results suggest that the preservation of a normal structural relationship between the neoplastic luminal epithelial and myoepithelial cells seems to be necessary for LM38-LP cells to develop into a differentiated tumor. However, we cannot rule out the influence of other non-identified cells that could be providing the nonmalignant stroma of LM38-LP papillary carcinomas, as recently shown in a human breast cancer [25].

Similar interactions between these two cells might also contribute to the capacity of LM38-LP cells to form duct-like structures when grown in suspension. Gudjonsson and colleagues recently suggested [28] that intact myoepithelial cells might have a key role in the control of mammary epithelium polarity. Furthermore, they found that tumor-derived non-neoplastic myoepithelial cells were unable to induce the formation of polarized acinus-like structures by normal luminal cells embedded in type I collagen, owing to an inability to produce laminin-1 [28]. Just as loss of polarity and disorganized growth are a hallmark of malignant transformation, the ability of LM38-LP cells to

form rather differentiated structures in suspension is at least an unusual finding, and deserves further study.

It has been proposed that fully differentiated normal myoepithelial cells exert a restrictive control on the proliferation of normal luminal and malignant breast cells [29]. Our results suggest that malignant myoepithelial cells present in LM38-LP cultures might also limit the proliferation of luminal cells under some conditions. In fact, the reduction in number and/or the major phenotypic changes suffered during culture by myoepithelial cells could be associated with the significantly higher growth rate of LM38-HP cultures either in monolayer or in three-dimensional spheroids *in vitro*. However, different behaviour was evident when cell growth was measured under more stringent conditions, because only the LM38-LP subline was able to form colonies when grown at low density. Moreover, the LM38-LP cells were less susceptible than LM38-HP cells to serum deprivation. *In vivo* tumor growth studies agreed with these latter results. In fact, when inoculated s.c. into syngeneic mice, LM38-LP cells showed higher tumorigenicity, shorter latency, and more rapid growth, in comparison with LM38-HP and LM38-D2 cells.

Although there is an apparent contradiction between *in vitro* and *in vivo* growth capacity of the LM38-HP cell line, the complex interactions occuring *in vivo* must be taken into account and deserve future study. Interestingly, when LM38-HP and LM38-D2 cells were co-cultivated and inoculated together, the resulting combined s.c. tumors showed a 2.8-fold size increase. These data support the hypothesis that M38 tumor growth depends on a reciprocal interplay between these two cell types.

The mechanisms involved in the dissemination and growth of tumor cells in lymph nodes are largely unknown in human breast cancer biology, probably owing to the lack of proper experimental models, as mentioned above. The fact that M38 and LM38-LP cells were able to colonize the lymph node, that this capacity was significantly diminished in LM38-HP cells and absent from the isolated myoepithelial clone, suggest that specific interactions between luminal and myoepithelial cells might be necessary. Interestingly, the ability to metastasize lung was also impaired in both LM38-HP cells and the myoepithelial clone. The co-inoculation experiments demonstrated a direct correlation between epithelial and myoepithelial interplay and lung metastatic capacity, but failed to recover regional lymph node colonization. Although a loss of tumor and metastatic growth capability could be attributed to a loss of function induced by prolonged cell culture, this is a rather controversial aspect in the literature. In this regard, in previous works we have reported an enhancement of the invasive and metastatic phenotype when continuous cell lines were established from spontaneous transplantable murine mammary tumors [19,30].

The metastatic cascade is a multistep process that involves the overexpression of proteolytic enzymes such as uPA and MMPs [21,31,32]. uPA initiates an enzymatic cascade, involving the activation of plasminogen to plasmin and of matrix metalloproteinases, which not only enable the degradation of the surrounding extracellular matrix but might also exert other roles in regulating cell proliferation and migration as well as angiogenesis [33,34]. To find some mechanistic explanation for the differences in the metastatic dissemination capacities of the different cell subpopulations studied, we analyzed the production of uPA and MMPs. All of our lines produced and secreted 48 kDa uPA, but the LM38-LP cell line secreted significantly higher uPA activity levels than LM38-HP cells and the isolated clone. Although we cannot exclude the possibility that the decrease in uPA production exhibited by LM38-HP cells was a consequence of the prolonged culture, it is possible that interaction between both cell types is necessary to produce elevated levels of this enzyme. The myoepithelial clone was evaluated between subcultures 9–15, thus eliminating prolonged culture as a cause of its lower uPA secretion.

Regarding MMPs, only the highly metastatic LM38-LP subline was able to secrete MMP-2. This interesting finding agrees with Kawamata and colleagues [35], who associated MMP-2 activity with the ability of a human oral-squamous-cancer cell line to disseminate to regional lymph nodes. In sum, we consider that these results allow us to propose that uPA and MMP-2 participate in the growth and metastatic capacity of the M38 tumor.

Concerning the nature of the interactions between M38 luminal and myoepithelial cells, our experiments suggest that the secretion and paracrine activity of soluble factors are probably not enough, because cross-treatment with CM did not modulate either the morphology or the growth pattern of any of the cultures. However, the secretion of labile soluble factors with a high turnover cannot be discounted. Interestingly, it was necessary to cultivate LM38-HP and LM38-D2 cells together for 36 hours to achieve differences in the co-inoculation experiments; these were not found in preliminary assays when co-injection without previous co-culture was used.

We do not know yet whether the different cell components of the M38 tumor, present both in primary cultures and in the LM38-LP subline, are the differentiated progeny of a single mutated stem cell or arose only after further mutation(s) of lineage-committed progenitor cells [20,36,37]. It is worth mentioning that the M38 tumor arose in a mammary gland of a pregnant BALB/c mouse, when both stem and already committed cycling cells (of both luminal and myoepithelial phenotypes) are usually found. Interestingly, beside the immunocytochemically defined epithelial and myoepithelial main components, other unidentified cells were also present in the LM38-LP cell line. Moreover, the LM38-HP subline presented a main subpopulation of small spindle cells, which could be an emergent third type of an otherwise insignificant subpopulation already present in LM38-LP cultures, or alternatively they could have evolved from the islet-forming epithelial cells, given that they present the same altered DNA ploidy.

A hypothesis to explain the repeated failure to isolate pure epithelial cells able to form islets of luminal phenotype by the limiting dilution cloning procedure is that they are probably almost terminally differentiated. In contrast, myoepithelial cells can be isolated with a high frequency as pure populations, and remain so after several passages *in vitro*, suggesting the presence of a clonogenic, committed and transformed myoepithelial progenitor in the LM38-LP cell line. Finally, it is quite probable that a transformed and as yet unidentified multipotent stem cell is also being isolated, because the clones that were initially formed from either small spindle cells or epithelioid-like cells quickly developed into mixed heterogenous cultures quite similar to the LM38-LP cell line. Other approaches, such as immunomagnetic sorting [14], should be employed to isolate either the transformed luminal cell or the putative transformed stem cell.

Conclusions
The underlying biology of the mammary epithelium is complex, and the distinct cellular compartments that give rise to cancers are not fully defined. Our data suggest that interactions between malignant epithelial cells with both luminal and myoepithelial phenotypes might be crucial in determining the differentiated histopathology and malignant behavior of the M38 mammary adenocarcinoma, including its unique capacity to colonize the draining lymph node. Thus we believe that this new model is a useful tool for analyzing the molecular mechanisms involved in both the initiation and the progression of breast cancer.

Competing interests
None declared.

References
1. Lakhani S, O'Hare M: **The mammary epithelial cell – Cinderella or ugly sister?** *Breast Cancer Res* 2001, **3:**1-4.
2. Deugnier MA, Teulière J, Faraldo M, Thiery JP, Glukhova MA: **The importance of being a myoepithelial cell.** *Breast Cancer Res* 2002, **4:**224-230.

3. Liu QY, Niranjan B, Gomes P, Gomm J, Davies D, Coombes C, Buluwela L: **Inhibitory effects of activin on the growth and morphogenesis of primary and transformed mammary epithelial cells.** *Cancer Res* 1996, **56:**1155-1163.

4. Rudland PS, Fernig DG, Smith JA: **Growth factors and their receptors in neoplastic mammary glands.** *Biomed Pharmacother* 1995, **49:**389–399.

5. Xiao G, Liu YE, Gentz R, sang QA, Ni J, Goldberg ID, Shi YE: **Suppression of breast cancer growth and metastasis by a serpin myoepithelium derived serine protease inhibitor expressed in the mammary myoepithelial cells.** *Proc Natl Acad Sci* 1999, **96:**3700-3705.

6. Nguyen M, Lee MC, Wang JL, Tomlinson JS, Shao ZM, Alpaugh ML, Barsky SH: **The human myoepithelial cell displays a multi-faceted anti-angiogenic phenotype.** *Oncogene* 2000, **19:**3449-3459.

7. Sternlicht MD, Kedeshian P, Shao ZM, Safarians S, Barsky SH: **The human myoepithelial cell is a natural tumor suppressor.** *Clin Cancer Res* 1997, **3:**1949–1958.

8. Rehm S: **Chemically induced mammary gland adenomyoepitheliomas and myoepithelial carcinomas of mice. Immunohistochemical and ultrastructural features.** *Am J Pathol* 1990, **136:**575-584.

9. Foschini MP, Eusebi V: **Carcinomas of the breast showing myoepithelial cell differentiation. A review of the literature.** *Virchows Arch* 1998, **432:**303–310.

10. Nagle RB, Bocker W, Davis JR, Heid HW, Kaufmann M, Lucas DO, Jarasch ED: **Characterization of breast carcinomas by two monoclonal antibodies distinguishing myoepithelial from luminal epithelial cells.** *J Histochem Cytochem* 1986, **34:**869–881.

11. Jones C, Nonni AV, Fulford L, Merrte S, Chaggar R, Eusebi B, Lakhani SR: **Analysis of ductal carcinoma of the breast with basaloid/myoepithelial cell differentiation.** *Br J Cancer* 2001, **85:**422-427.

12. Pechoux C, Gudjonsson T, Ronnov-Jessen L, Bissell MJ, Petersen OW: **Human mammary luminal epithelial cells contain progenitors to myoepithelial cells.** *Dev Biol* 1999, **206:**88–99.

13. Böcker W, Moll R, Poremba C, Holland H, van Diest P, Dervan P, Bürger H, Wai D, Diallo Rl, Brandt B, Herbst H, Schmidt A, Lerch M, Buchwallow I: **Common adult stem cells in human breast give rise to glandular and myoepithelial cell lineages: a new cell biological concept.** *Lab Invest* 2002, **82:**737-746.

14. Gudjonsson T, Villadsen R, Nielsen H, Rønnov-Jessen L, Bissell MJ, Petersen OW: **Isolation, immortalization and characterization of a human breast epithelial cell line with stem cell properties.** *Genes Dev* 2002, **16:**693-706.

15. Jones C, Foschini MP, Chaggar R, Lu YJ, Wells D, Shipley JM, Eusebi V, Lakhani SR: **Comparative genomic hybridization analysis of myoepithelial carcinoma of the breast.** *Lab Invest* 2000, **80:**831–836.

16. Cardiff RD, Anver MR, Gusterson BA, Henninghausen L, Jensen RA, Merino MJ, Rehm S, Russo J, Tavassoli FA, Wakefield LM, Warad JM, Green JE: **The mammary pathology of genetically engeneered mice: the consensus report and recommendations from the Annapolis meeting.** *Oncogene* 2000, **19:**968-985.

17. Manzur T, Diament M, Vauthay L, Stillitani I, García C, Fontanals A, Klein S: **Tumores murinos espontáneos de experimentación en el Instituto de Oncología 'Angel H. Roffo'. Animales de Experimentación.** *Rev Hispanoamer* 1998, **4:**25-26.

18. Alonso DF, Farías EF, Bal de Kier Joffé ED: **Urokinase-type plasminogen activator activity released by clonal tumor cell populations isolated along the growth of a murine mammary adenocarcinoma.** *J Exp Clin Cancer Res* 1994, **13:**211-216.

19. Urtreger A, Ladeda V, Puricelli L, Rivelli A, Vidal MCC, Sacerdote de Lustig E, Bal de Kier Joffé E: **Modulation of fibronectin expression and proteolytic activity associated to the invasive and metastatic phenotype in two new murine mammary tumor cell lines.** *Int J Oncol* 1997, **11:**489-496.

20. Chepko G, Smith GH: **Three division-competent structurally-distinct cell populations contribute to murine mammary epithelial renewal.** *Tissue Cell* 1997, **29:**239-253.

21. Aguirre Ghiso J, Alonso A, Farías E, Gómez D, Bal de Kier Joffé E: **Deregulation of the signaling pathways controlling urokinase production. Its relationship with the invasive phenotype.** *Eur J Biochem* 1999, **263:**295-304.

22. Rosen PP: **Invasive mammary carcinoma.** In *Diseases of the Breast*. Edited by Harris JR, Lippman ME, Morrow M, Hellman S. Philadelphia: Lippincott Raven Publishers; 1996:393-444.

23. Rønnov-Jessen L, Petersen O, Bissell M: **Cellular changes involved in conversion of normal to malignant breast: importance of the stromal reaction.** *Physiol Rev* 1996, **76:**69-125.

24. Petersen OW, van Deurs B: **Preservation of defined phenotypic traits in short-term cultures human breast carcinoma derived epithelial cells.** *Cancer Res* 1987, **47:**856-866.

25. Petersen OW, Lind Nielsen H, Gudjonsson T, Villadsen R, Rank F, Niebuhr F, Bissell M, Rønnov-Jessen L: **Epithelial to mesenchymal transition in human breast cancer can provide a nonmalignant stroma.** *Am J Pathol* 2003, **162:**391-402.

26. Perou CM, Sorlie T, Eisen MB, Van de Rijn M, Jeffrey SS, Rees CA, Pollack JR, Ross DT, Johnsen H, Akslen LA, Fluge O, Pergamenschikov A, Williams C, Zhu SX, Lonning P E, Borresen-Dale AL, Brown PO, Botstein D: **Molecular portraits of human breast tumours.** *Nature* 2000, **406:**747–752.

27. Gruvberger S, Ringner M, Chen Y, Panavally S, Saal LH, Borg A, Ferno M, Peterson PS, Meltzer PS: **Estrogen receptor status in breast cancer is associated with remarkably distinct gene expression patterns.** *Cancer Res* 2001, **61:**5979–5984.

28. Gudjonsson T, Rønnov-Jessen L, Villadsen R, Rank F, Bissell MJ, Petersen OW: **Normal and tumor-derived myoepithelial cells differ in their ability to interact with luminal breast epithelial cells for polarity and basement membrane deposition.** *J Cell Sci* 2002, **115:**39-50.

29. Shao ZM, Nguyen M, Alpaugh ML, O'Connel JT, Barsky SH: **The human myoepithelial cell exerts antiproliferative effects on breast carcinoma cells characterized by p21 WAF1/CIP1 induction, G2/M arrest and apoptosis.** *Exp Cell Res* 1998, **241:**394-403.

30. Alonso DF, Farías EF, Urtreger AJ, Ladeda VE, Vidal MCC, Bal de Kier Joffé ED: **Characterization of F3II, a sarcomatoid mammary carcinoma cell line originated from a clonal subpopulation of a mouse adenocarcinoma.** *J Surg Oncol* 1996, **62:**288-297.

31. Danø K, Romer J, Nielsen BS, Bjorn S, Pyke C, Rygaard L, Lund LR: **Cancer invasion and tissue remodeling-cooperation of protease systems and cell types.** *APMIS* 1999, **107:**120-127.

32. Ossowski L: **Invasion of connective tissue by human carcinoma cell lines: requirement for urokinase, urokinase receptor and interstitial collagenase.** *Cancer Res* 1992, **52:**6754-6760.

33. Chambers A, Matrisian L: **Changing views of the role of matrix metalloproteinases in metastasis.** *J Natl Cancer Inst* 1997, **89:**1260-1270.

34. Ossowski L, Aguirre Ghiso J: **Urokinase receptor and integrin partnership: coordination of signaling for cell migration, adhesion and growth.** *Curr Opin Cell Biol* 2000, **12:**613-620.

35. Kawamata H, Nakashiro K, Uchida D, Harada K, Yoshida H, Sato M: **Possible contribution of active MMP 2 to lymph-node metastasis and secreted cathepsin L to bone invasion of newly established human oral-squamous-cancer cell lines.** *Int J Cancer* 1997, **70:**120-127.

36. Dontu G, Abdallah WM, Foley JM, Jackson KW, Clark MF, Kawamura MJ, Wicha MS: **In vitro propagation and transcriptional profiling of human mammary/progenitor cells.** *Genes Dev* 2003, **17:**1253-1270.

37. Kordon EC, Smith GH: **An entire functional mammary gland may comprise the progeny from a single cell.** *Development* 1998, **125:**1921-1930.

Correspondence

Elisa Bal de Kier Joffé, Area Investigación, Instituto de Oncología 'Angel H Roffo', Avda San Martín 5481, C1417DTB Buenos Aires, Argentina. Tel: +5411 4504 7884; fax: +5411 4580 2811; e-mail: elisabal@fmed.uba.ar